The paradoxical effects of chronic intra-amniotic *Ureaplasma parvum* exposure on ovine fetal brain development.

Ruth Gussenhoven[a,b], Daan R.M.G. Ophelders[a,b], Matthew W. Kemp[c], Matthew S. Payne[c], Owen B. Spiller[d], Michael L. Beeton[e], Sarah Stock[c,f] , Bertha Cillero-Pastor[g], Florian P.Y. Barré[g], Ron M.A. Heeren[g], Lilian Kessels[a], Bas Stevens[a], Bart P. Rutten[b,h], Suhas G. Kallapur[i], Alan H. Jobe[i] , Boris W. Kramer[a,b,j], Tim G.A.M. Wolfs[a,j,k,#]

a Department of Pediatrics, Maastricht University Medical Center, Maastricht, the Netherlands

b School for Mental Health and Neuroscience (MHeNs), Maastricht University Medical Center, Maastricht, the Netherlands

c School of Women's and Infants' Health, the University of Western Australia (M550), Crawley, WA, Australia

d Institute of Molecular and Experimental Medicine, Cardiff University, School of Medicine, Cardiff, United Kingdom

e Department of Biomedical Sciences, Cardiff Metropolitan University, Cardiff, United Kingdom

f Tommy's Centre for Maternal and Fetal Health, MRC Centre for Reproductive Health, University of Edinburgh Queen's Medical Research Institute, Edinburgh, United Kingdom

g The Maastricht Multimodal Molecular Imaging Institute (M4I), Maastricht University Medical Center, Maastricht, the Netherlands

h Department of Psychiatry and Neuropsychology, Maastricht University Medical Center, Maastricht, the Netherlands

i Division of Neonatology/Pulmonary Biology, The Perinatal Institute, Cincinnati Children's Hospital Medical Center, University of Cincinnati, Cincinnati, OH, USA

j School of Oncology and Developmental Biology (GROW), Maastricht University Medical Center, Maastricht, the Netherlands

k Department of Biomedical Engineering, Maastricht University Medical Center, Maastricht, the Netherlands

#Corresponding author:

Tim G.A.M. Wolfs

Maastricht University Medical Center

Department of Pediatrics

P. Debyelaan 25

6202 AZ Maastricht, The Netherlands

Ph: +31-43-388-2232 / Fax: +31-43-387-5246

E-mail: tim.wolfs@maastrichtuniversity.nl

Running head

Ureaplasma exposure and fetal brain development

Keywords

Ureaplasma parvum, intra-amniotic inflammation, chorioamnionitis, fetal brain, sheep, double-hit, preterm birth

Abstract

Chorioamnionitis is associated with adverse neurodevelopmental outcomes in preterm infants. *Ureaplasma* spp. are the microorganisms most frequently isolated from the amniotic fluid of women diagnosed with chorioamnionitis. However, controversy remains concerning the role of *Ureaplasma* spp. in the pathogenesis of neonatal brain injury. We hypothesize that re-exposure to an inflammatory trigger during the perinatal period might be responsible for the variation in brain outcome of preterms following *Ureaplasma* driven chorioamnionitis. To investigate these clinical scenarios, we performed a detailed multi-modal study in which ovine neurodevelopmental outcomes were assessed following chronic intra-amniotic *Ureaplasma parvum* (UP) infection, either alone or combined with subsequent lipopolysaccharide (LPS) exposure.

We show that chronic intra-amniotic UP exposure during the second trimester provoked a decrease of astrocytes, increased oligodendrocyte numbers and elevated 5-methylcytosine levels. In contrast, short-term LPS exposure before preterm birth induced increased microglial activation, myelin loss, elevation of 5-hydroxymethylcytosine levels and lipid profile changes. These LPS-induced changes were prevented by chronic pre-exposure to UP (preconditioning).

These data indicate that chronic UP exposure provokes dual effects on preterm brain development *in utero*. On one hand, prolonged UP exposure causes detrimental cerebral changes which may predispose to adverse postnatal clinical outcomes. On the other, chronic intra-amniotic UP exposure preconditions the brain against a second inflammatory hit. This study demonstrates that microbial interactions, timing and duration of inflammatory insults will determine the effects on the fetal brain. Therefore, this study helps to understand the complex and diverse postnatal neurological outcomes following UP driven chorioamnionitis.

Introduction

Neonatal brain injury acquired during pregnancy remains a major cause of adverse neurodevelopmental outcomes throughout life [1, 2]. Chorioamnionitis which is defined as a microbial invasion and infection of the amniotic cavity is one of the most important risk factors for adverse neurodevelopmental outcomes of the newborn [3, 4]. *Ureaplasma* spp. are the most common isolated micro-organisms associated with chorioamnionitis [5]. Clinical recognition of amniotic fluid infections is challenging given its asymptomatic course despite sustained fetal exposure to intrauterine inflammation, particularly during the critical period of fetal brain development [6].

Intra-amniotic exposure to *Ureaplasma* spp. is associated with development of fetal and neonatal brain injury [7-10]. Clinical data show that there is an increased risk for intraventricular hemorrhage and impaired neurodevelopmental outcomes later in life after intra-amniotic *Ureaplasma* spp. exposure [7, 9, 10]. This association was confirmed by Normann et al. who showed that intra-amniotic *Ureaplasma parvum* (UP) exposure resulted in increased microglial activation, delayed myelination, and disturbed cortical development of the fetal murine brain [11]. In contrast, clinical studies reported that antenatal exposure to *Ureaplasma* spp. and brain injury did not correlate [12, 13]. Diversities in microbial interplay, timing, duration and severity of the inflammatory response after onset of chorioamnionitis are considered to determine the neurodevelopmental outcome which most likely explains the considerable differences in antenatal UP exposure and brain injury incidences among studies [14, 6]. In particular, the onset of cerebral inflammation during the brain's most vulnerable period from 23 to 32 weeks of gestation can have detrimental consequences for the fetal brain, particularly white matter damage. Multiple animal models demonstrate that the brain becomes more (i.e. sensitization) or less (i.e. preconditioning)

susceptible to a second injurious hit following pre-exposure to inflammation [15, 16]. Besides cerebral inflammation, epigenetic mechanisms (such as DNA methylation and DNA hydroxymethylation) may mediate the processes leading to brain injury in response to environmental challenges *in utero* [17]. In line, DNA-methylation levels in genes involved in growth and development are found to be increased in premature infants with chorioamnionitis compared with infants without chorioamnionitis [18].

Moreover, alterations of phospholipids which are highly abundant in the brain and play important functions in cell membrane formation, as energy reservoirs and as precursors for second messengers (i.e. arachidonic acid (AA)) [19] have been implicated in multiple brain pathologies. In particular, changes in lipid metabolism, as seen in lysosomal storage diseases, can cause severe impaired brain function with lipids accumulating within the brain [20].

Detailed investigations of the interactions between different infectious triggers and the timing and duration of inflammatory exposures in the context of a polymicrobial syndrome such as chorioamnionitis is essential to understanding the complex and diverse neurodevelopmental outcomes after birth. We therefore investigated the effects of chronic intra-amniotic UP exposure in the presence or absence of a second (acute) inflammatory stimulus on fetal neurodevelopment. We used a well-established translational ovine model of intrauterine inflammation in which fetuses were chronically exposed to intra-amniotic UP, followed by acute exposure to *Escherichia coli*-derived lipopolysaccharide (LPS). Cerebral outcome was studied by analyzing inflammation, structural injury, epigenetic markers and lipid profile composition of the fetal brain.

Methods

Animal experiments

The animal procedures were performed with approval of the animal ethics committee of the University of Western Australia (Perth, Australia).

Thirty-seven date-mated Merino ewes were randomly assigned to study groups of 5-7 animals. Fetuses of either sex were used. Ewes received an ultrasound-guided intra-amniotic injection of culture media (2 mL) as control or strain HPA5 of *Ureaplasma parvum* (UP) serovar 3 (2×10^5 colony changing units (CCU)) at 80 days of gestation (term ~ 150 days). To minimize any inflammatory effects from culture media, both UP and control injections were created from stock cultures/sterile media diluted 1:100 in sterile saline. To assess the effect of an additional inflammatory hit following long-term pre-exposure with UP, both groups received a second intra-amniotic injection of 10mg *Escherichia coli*-derived LPS (O55:B5; Sigma-Aldrich, St. Louis, MO) at 2 or 7 days before preterm delivery at 122±2 days of gestation or an equivalent dose of saline (SAL; controls) (Fig. 1).

Data acquisition and analysis

All fetuses were surgically delivered via Caesarean section at 122±2 days of gestation (equivalent of 32–34 weeks human gestation) and euthanized with intravenous pentobarbitone (100 mg/kg) immediately after birth. Amniotic fluid (AF), blood and cerebrospinal fluid (CSF) were collected at delivery and cultures for UP were performed. Brains were immersion fixed in 4% paraformaldehyde.

Culture analysis of UP infection

Samples of amniotic fluid (1 ml) collected by amniocentesis at LPS or control saline injection, as well as plasma, CSF and amniotic fluid collected at Caesarean-section delivery were cultured for UP growth as previously described [21]. For each animal, twenty microliters of biological fluid was serially diluted 1:10 in Ureaplasma Selective Medium (Mycoplasma Experience plc., Reigate, UK) in triplicate for each sample and incubated at 37°C. Assays were performed in 96 well plates and bacterial growth was quantified by the titration of the urease activity (conversion of urea to ammonium ions leading to pH color change). Plates were observed until bacteria-mediated color change ceased and the titration of the bacteria present determined.

Analysis of IL-6 concentration

The pro-inflammatory cytokine IL-6 was measured in fetal plasma as marker for systemic inflammation using a sheep-specific sandwich enzyme-linked immunosorbent assay (ELISA). Briefly, a mouse-anti-ovine monoclonal antibody (MAB1004, Millipore, Darmstadt, Germany, working concentration 1:200) was the coating antibody. Plasma samples (100 µL) were loaded per well in duplicate and incubated for 2 hours at room temperature. Incubation with the detection antibody (rabbit-anti-ovine IL-6, AB1839, Millipore, Darmstadt, Germany, working concentration 1:500) was performed for 60 minutes, followed by incubation for 30 minutes with 100 µL of a goat-anti-rabbit-HRP (Jackson ImmunoResearch Laboratories Inc, West Grove, PA, USA, working concentration 1:500). After washing, incubation with 3,3′,5,5′-tetramethylbenzidine (TMB) substrate solution for 15 minutes. The reaction was stopped by addition of 50 µL 2N sulfuric acid. The optical density (OD) was measured using a micro-plate reader at 450 nm. Concentrations were expressed relative to a standard curve of ovine IL-6 recombinant protein (ImmunoChemistry Technologies, Bloomington, MN, USA).

Histology and immunohistochemistry

After fixation, the right hemisphere was divided into four defined anatomical regions. The region of the posterior hippocampus/mid-thalamus was embedded in paraffin and serial coronal sections (4 µm) were cut with a Leica RM2235 microtome. At this level, we analyzed the hippocampus and cerebral white matter for inflammatory and structural changes since these regions are most affected following intra-uterine infection at this developmental stage [22]. Four slides per staining per animal were used (every 10^{th} consecutive slide) for immunohistochemical analysis. Hematoxylin and eosin (H&E) staining was performed for morphological and anatomical analysis. Adjacent sections were stained as previously described with a rabbit anti-ionized calcium binding adaptor molecule 1 (IBA-1) antibody (Wako Pure Chemical Industries, Osaka, Japan) for microglia, a rabbit anti-glial fibrillary acidic protein (GFAP) antibody (DAKO Z0334) for astrocytes, a rat anti-myelin basic protein (MBP) antibody (Merck Millipore, MAB386) for myelin sheaths, a rabbit anti-oligodendrocyte transcription factor 2 (Olig2) antibody (Millipore, AB9610) for oligodendrocyte lineage cells, a rabbit anti-myeloperoxidase (MPO) (DAKO, A0398) for neutrophils, a mouse anti-cluster of differentiation (CD) 68 (DAKO, M0718) for active microglia/phagocytizing macrophages, a rabbit anti-CD3 (DAKO A0452) for T-lymphocytes and a mouse anti-5-Methylcytosine (5-mc) (Genway GWB-CB561B) and rabbit anti-5-Hydroxymethylcytosine (5-hmc) (Active Motif, 39769) were used as epigenetic markers.

Endogenous peroxidase activity was inactivated with 0.3% H_2O_2 treatment (or 1% H_2O_2 for 5-mc and 5-hmc). Antigen retrieval was performed by microwave boiling of tissue sections in citrate buffer (pH 6.0). Nonspecific binding was blocked by incubation with bovine, goat or donkey serum in PBS. Sections were incubated overnight at 4°C with the diluted primary antibody (5-hmc 1:2500; IBA-1, GFAP and MBP 1:1000; 5-mc 1:500; Olig2, MPO 1:200). The following day sections were incubated with the specific secondary antibody and staining was enhanced with a Vectastain ABC

peroxidase Elite kit (Vector Laboratories Inc, Burlingame, CA) and (nickel) 3,3'-diaminobenzidine (DAB) staining. If required, appropriate background staining was performed.

Matrix assisted laser desorption ionization mass spectrometry imaging

A more detailed molecular analysis of the cerebral tissue was done by matrix assisted laser desorption ionization mass spectrometry imaging (MALDI-MSI) to map variations in lipid profiles of the white and grey matter. MALDI-MSI to image lipid distribution can be invaluable in understanding complex lipid changes and it has been used to study these molecular patterns in models of brain injury [23]. With MALDI-MSI we avoid all extraction and purification steps for lipid analysis while retaining their spatial distribution. For this technique, post fixation tissues of controls, 42UP, 2LPS and UP&LPS groups were frozen in liquid nitrogen and subsequently samples were cryo-sectioned (10 µm thickness) in a cryostat (Leica CM3050S), deposited on indium tin oxide high-conductive slides (Delta Technologies, US), and stored at –20°C. Subsequently, the matrix solution consisting of norharman (7 mg/ml) in 2:1 chloroform:methanol was sprayed on top of the tissue section by a vibrational sprayer (Suncollect; SunChrom, Germany) for positive ion mode and 9-aminoacridine (10 mg/mL) in 70% ethanol for negative ion mode MALDI-MSI analysis. Digital optical scans of all tissue sections were obtained prior to MALDI-MSI experiments using a 2,400 dots per inch desktop scanner. The resulting digital images were imported into the MALDI Imaging HDI software v1.4 (Waters Corporation). A MALDI-quadrupole time-of-flight SYNAPT HDMS G2Si system (Waters Corporation) operating with a 200-Hz Nd:YAG laser was configured to acquire data in positive and negative V-reflectron mode. Data were acquired at a raster size of 100 by 100 µm. Instrument calibration was performed using a standard calibration solution of red phosphorus.

Principal components analysis (PCA) and discriminant analysis (DA) were used to investigate spectral similarities and differences between all samples. PCA was performed as a data compression and noise filtering step before application of DA, only 1/4 of the functions (216) were used as input for DA. In short, PCA is an unsupervised statistical method that aims at pooling a maximum amount of variance in a minimum number of independent variables. Data pre-treatment, PCA and DA were performed using our in-house built ChemomeTricks toolbox for MATLAB version 2014a (The MathWorks, Natick, MA, USA). The peak assignments were performed according to the bibliography and LIPID MAPS software (http://www.lipidmaps.org/).

Qualitative analysis

H&E-stained sections were analyzed by two independent investigators and a neuropathologist, blinded for the experimental set up, to assess overall brain structure and inflammatory changes. The sections were examined for the presence of gliosis, hemorrhages, (cytotoxic) edema and structural damage, including cyst formation.

Immunohistochemical analysis

Immunohistochemical stainings were analyzed using a light microscope (Leica DM2000) equipped with Leica QWin Pro version 3.4.0 software (Leica Microsystems, Mannheim, Germany). Regions of interest of the white matter and hippocampus were defined as previously described [24]. These regions were chosen since they are most affected by intra-uterine infections at this developmental stage. In the white matter 4-6 adjacent images were taken at 100x magnification and from the hippocampus one image at 20x magnification was taken. To assess regional vulnerability within the hippocampus separate images were taken at 200x magnification of the Cornu Amonis (CA) 1&2, 3 and 4 and the dentate gyrus (DG). Area fractions of IBA-1, GFAP, MBP, 5-mc and 5-hmc

expression were determined using a standard threshold to detect positive staining with Leica QWin Pro V 3.5.1 software (Leica, Rijswijk, the Netherlands). Regions of interest were delineated in the image with large blood vessels and artefacts excluded from analysis. Since the level of DNA methylation and hydroxymethylation can differ per cell, the integrated density of 5-mc and 5-hmc was calculated by multiplying the area fraction by the mean gray value, and these values were normalized to the data of the control group as previously described by Lardenoije et al [25]. In addition to area fraction analysis, IBA-1 and GFAP positive cells were counted in 3 fields of view within the regions of interest at a magnification of 400x. The Olig2 positive cells were counted using Qwin software and expressed as cells/mm2. MPO positive cells were counted focusing on the cerebral vasculature, meninges and choroid plexus. To quantify the density (cells per mm2) of MPO-, CD68- and CD3-positive cells, representative images of the choroid plexus present in the lateral ventricles aligning the hippocampus were counted using ImageJ software (Rasband, W.S., Image J US National Institutes of Health, Bethesda, Maryland, USA; RRID:SCR_003070). The images were acquired and analyzed by an independent observer who was blinded to the experimental groups.

Data analysis.

All values are shown as means with 95% confidence interval or standard deviations with significance level at $p < 0.05$. Comparison between different experimental groups was performed with analysis of variance (ANOVA) or with a random intercept mixed model in case of repeated measurements per animal (e.g., different sections per brain). We applied log-transformation to obtain normal distributed data when data or variables were positively skewed before statistical testing. Statistical analysis was performed with IBM SPSS Statistics Version 22.0 (IBM COrp.,

Armonk, NY, USA; SPSS, RRID: SCR_002865). Considering the relative low number of animals per group, we have depicted the exact p-values in Fig. 4-6.

Results

Ureaplasma parvum cultures and detection

Chronic UP infection in animals inoculated at 80 days of gestation was confirmed by culture of amniotic fluid at the time of subsequent LPS or saline injections by amniocentesis (Fig. 2). No significant differences in the UP levels were observed between the three groups (42UP 1.1±0.8 $x10^6$ CCU/ml; UP&2LPS 1.1±0.8 $x10^7$ CCU/ml; UP&7LPS 9.4±0.7 x 10^6 CCU/ml). Cultures of amniotic fluid at time of delivery were positive for UP in all experimentally infected animals except one of the animals of the UP&7LPS group. No endogenous UP growth was observed in the amniotic fluid of animals that were not inoculated with UP (SAL, 2LPS and 7LPS groups). No UP growth in CSF or plasma was observed for any animal.

Animal characteristics

Overall, no sex differences in susceptibility were observed in all readouts. LPS exposure for 2 days decreased the body weight (SAL vs. 2LPS; $p = 0.002$) and increased brain-to-body ratio (SAL vs. 2LPS; $p = 0.038$) compared to controls (Table 1). These significant changes were not observed in animals that were chronically exposed to UP prior to 2 days of LPS exposure (UP&2LPS). Moreover, no change in brain weight or brain-to-body ratio was observed in animals of the 42UP, 7LPS and UP&7LPS groups compared to control animals.

Circulatory pro-inflammatory cytokine levels

Elevated plasma IL-6 concentrations were found in 50% (3/6) of the 2 day LPS exposed animals and in 20% (1/5) of the 42 days UP and 2 days LPS exposed animals when compared to controls (Fig. 3). Plasma IL-6 concentrations in the SAL, 42UP, 7LPS and UP&7LPS animals were not detectable.

Structural analysis of the brain

Qualitative analysis of H&E stained sections revealed increased cell densities in the gyral crest of the white matter which primarily consisted of glial cells. These gliotic foci were most prominent in 3/6 (50%) of the 2d LPS exposed animals. Furthermore, in 1/6 (16%) of the 42d UP exposed animals and in 1/6 (16%) of the 7d LPS exposed animals these gliotic foci were present. Control animals and animals of the UP & LPS combined groups had mild to no gliotic foci. No evidence of structural changes including intraventricular hemorrhages and cystic lesions were present in any of the experimental groups.

Dual effects of chronic UP infection on cerebral development.

The neuroinflammatory changes, as indicated by the more pronounced presence of gliotic foci in the 2d LPS exposed animals were further evaluated by cell counts and area fraction analysis of the microglial marker IBA-1 and astrocytic marker GFAP in the cerebral white matter and hippocampus. Chronic intra-amniotic exposure to UP decreased GFAP immunoreactivity (IR) (SAL vs. 42UP; $p = 0.020$) and the number of astrocytes (SAL vs. 42UP; $p = 0.100$), compared to controls (Fig. 4). IBA-1 IR and IBA-1 positive cell numbers remained unaltered following chronic intra-amniotic UP exposure (Fig. 4). In contrast, acute exposure to LPS increased IBA-1 IR (SAL vs. 2LPS; $p = 0.008$) and the number of IBA-1 positive cells (SAL vs. 2LPS; $p = 0.036$) in the

cerebral white matter (Fig. 4). In addition, morphological analysis revealed a higher density of amoeboid microglia present in the white matter after 2 days of LPS exposure (Fig. 4 inserts). However, if the animals were chronically exposed to UP prior to LPS, no IBA-1 IR or IBA-1 positive cell increase was observed in the cerebral white matter at 2 or 7 days post-LPS challenge (Fig. 4d&f). Equally, LPS administration did return GFAP IR in chronically UP infected animals to control levels (Fig. 4c). This preconditioning effect of UP was also found in the hippocampus in which an increase of IBA-1 IR was found at 2 and 7 days following LPS exposure but not in the groups with pre-exposure to UP (SAL vs. 2LPS; $p = 0.002$ and SAL vs. 7LPS; $p = 0.000$) (data not shown). No changes of GFAP IR or GFA positive cell numbers were found following LPS exposure in the white matter (Fig. 4) and in the hippocampus (data not shown).

Since the choroid plexus is primarily dominated by macrophages, T-lymphocytes and dendritic cells for continuous immune surveillance, and the resolution of cerebral inflammation [26] we analyzed the distribution of CD68+ macrophages, CD3+ lymphocytes and MPO+ neutrophils within the choroid plexus. MPO-positive cells tended to be increased following 7d LPS exposure compared to control animals and this increase was prevented by pre-exposure to 42d UP (SAL vs. 7LPS; $p = 0.086$) (Tabel 2). In line, this increase in MPO-positive cells at 7d post LPS exposure was accompanied by a decrease in IBA-1 IR in the cerebral white matter compared to 2d LPS exposed animals. No differences in CD68 and CD3- positive cells were found in the choroid plexus. No CD3- and MPO-positive cells were detected in the brain parenchyma.

White matter injury was studied by assessing the densities of mature (MBP) and overall (Olig2) oligodendrocytes in the cerebral white matter. An apparent increase in Olig2 positive cells was found for all groups relative to control levels; however, this only reached significance for chronically UP-infected animals (SAL vs. 42UP; $p = 0.012$) and animals exposed to LPS for 2 days (SAL vs. 2LPS; $p = 0.037$) (SAL vs. 7LPS; $p = 0.211$, SAL vs. 42UP&2LPS; $p = 0.558$, SAL vs.

42UP&7LPS; p = 0.467) (Fig. 5c). In addition, MBP IR tended to be decreased at 42d following UP exposure (SAL vs. 42UP; p = 0.097) (Fig. 5). Short term LPS exposure for 2 days resulted in a decrease of MBP IR within regions of overt microgliosis (SAL vs. 2LPS; p = 0.001) which was prevented by pre-exposure to UP. At 7d of LPS exposure no changes in MBP IR were found (2LPS vs. 7LPS; p = 0.000).

We analyzed 5-mc and 5-hmc integrated density as epigenetic markers for DNA-methylation in the dentate gyrus of the hippocampus. We focused our analysis on the dentate gyrus since this is the region in the hippocampus were neurogenesis takes place and DNA methylation and demethylation are important contributors to this process [27, 28]. Both short term LPS exposure as well as chronic UP exposure resulted in an increase of the gene repression marker 5-mc integrated density compared to controls (SAL vs. 2LPS; p = 0.008 and SAL vs. 7LPS; p = 0.002 and SAL vs. 42UP; p = 0.008) (Fig. 6). The increase in 5-mc following LPS exposure tended to be prevented by pre-exposure to UP. An increase in transcription activation marker 5-hmc integrated density was only found in 2d LPS exposed animals compared to controls which was prevented by pre-exposure to UP (SAL vs. 2LPS; p = 0.000; 2LPS vs. 7LPS; p = 0.000) (Fig. 6).

Accumulation of lipids and changes in the white and grey matter lipid profile following acute LPS exposure is prevented by pre-exposure to UP.

We demonstrated with MALDI-MSI unique regional differences of the lipid composition in the preterm ovine brain between animals from the control, 42UP, 2LPS and UP&LPS group. Fig. 7 shows the reconstructed image that represents the molecular differences of lipids between white (red area) and grey matter (green area). The lipid composition, characteristic for healthy white and grey matter of the preterm brain was not altered following chronic UP exposure (Fig. 7a-c). In

particular, in the white matter of control and 42UP animals, typical tentative assigned *m/z* values of different phosphocholine (PC) species such as *m/z* 782.5 PC 34:1+Na^+, *m/z* 810.5 PC 36:1+Na^+ or sphingomyelin *m/z* 725.5 SM 34:1+Na^+ are found which are known to be representative for the white matter [29, 30] (Fig. 7c). *m/z* 756.5 PC 32:0+Na^+ which is a characteristic grey matter lipid [31], were detected in the grey matter of control and 42UP animals, demonstrating that control and chronic UP exposed animals had a similar and constitutive lipid profile.

Mosaic PCA-images demonstrated that short-term LPS exposure resulted in lipid accumulation in the white matter and diffusion of white matter specific molecular patterns into the grey matter and vice versa (Fig. 7d-i; Principal component 4 & 6). These changes were reduced when LPS exposure was preceded by 42 days of UP infection (Fig. 7e & h). In particular, the abundance of the white matter specific component *m/z* 725.5 in the grey matter of LPS exposed animals was not present in the grey matter of control or UP animals (Fig. 7g-i; negative spectrum of principal component 6). Whereas, *m/z* 734.5 PC 32:0+H^+ was accumulated in the grey matter of LPS animals (negative spectrum of principal component 4), and increased in the white matter (positive spectrum of principal component 6). In addition, principal component 6 showed that other peaks such as *m/z* 760 PC 34:1+H^+ accumulate in the white matter at 2d of LPS exposure which did not correspond with the pattern seen in our controls and those from others [29] in which these peaks were evenly distributed.

Other lipid species including phosphatidylinositols (PI) and sulfatide (SF) can be identified using the negative ion mode in MALDI-MSI. Regions of interest corresponding to the white matter were selected based on the results with the positive ion mode. The DF1 (Fig. 8a) reveals that the highest differences are observed between the control (negative scores) and LPS group (positive scores). The UP&LPS group had negative scores and therefore possessed a molecular composition more similar to the control group. The DF1 spectrum (Fig. 8b) shows the lipid composition of the white

matter of the 2 days of LPS exposed animals. This spectrum showed that LPS exposure reduced the amount of tentative assigned sulfatide (SF) species such as *m/z* 806.5 SF 18:0-H^-, *m/z* 888.6 SF 24:1-H^-, *m/z* 890.6 SF 24:0-H^-, which were described as lipids characteristic of white matter [29]. These species were mainly present in the white matter of control, UP and UP&LPS groups (spectrum not shown) whereas *m/z* 885.5 PI 38:4-H^- or *m/z* 718.6 PC 31:0-H^- were representative of the white matter in animals of the 2LPS group (fig.8b).

Discussion

Chronic intra-amniotic *Ureaplasma parvum* (UP) exposure decreased GFAP immunoreactivity (IR) and increased Olig2 positive cells and 5-methylcytosine (5-mc) IR in the brain. These changes have potential clinical implications postnatally.

The observed decrease of GFAP IR and number of astrocytes (GFAP+ cells) at 42d of UP exposure is important since these cells possess several essential functions in brain development including regulation of the extracellular glutamate homeostasis, providing structural and metabolic support to surrounding cells (e.g. oligodendrocytes) and modulate neuronal connections [32]. Changes in astrocyte function or density result in altered neurological outcomes. In particular, altered astrocyte protein expression (GFAP) and disrupted astrocyte maturation have been implicated in the pathogenesis of neurodevelopmental disorders such as autism and cerebral palsy [33, 34]. Moreover, Sharma et al. [35] showed that LPS injection in the spinal cord of rodents decreased astrocytes which was followed by hypomyelination. This suggests that white matter injury, a hallmark of preterm brain injury, can still occur in these fetuses considering the loss of GFAP IR at 42d post UP exposure. Collectively, the astrocyte cell and protein loss in our study indicates that

chronic UP exposure during the second trimester of gestation predisposes to brain pathologies that are often seen in newborns.

Second, the increase of oligodendrocyte lineage cells, as seen following 42d of UP exposure might indicate replenishment of oligodendrocytes upon initial loss in the acute phase following UP exposure [36]. Importantly, UP was administered at 80d of gestation which is the premyelinating stage of brain development with abundant vulnerable immature pre-oligodendrocytes, sensitive to glutamate receptor induced injury [37]. Interestingly, the mature oligodendrocytes tended to be decreased following chronic UP exposure. Given these combined findings of increased Olig2+ cell numbers and reduced MBP+ IR, it iss tempting to speculate that this indicates a maturation arrest of oligodendrocyte progenitor cells, a key feature of white matter injury of preterms [38-40]. This oligodendrocyte maturation arrest can be linked to the decreased astrocytes that we found in this study. Astrocytes are essential contributors to extracellular glutamate homeostasis which will be disturbed by a loss of astrocytes [32]. Since immature oligodendrocytes are particularly vulnerable to glutamate receptor induced injury, this can lead to oligodendrocyte injury [37]. In addition, oligodendrocytes rely on astrocytes for their metabolic support via gap junctions [41]. Failure of metabolic support for oligodendrocytes following astrocyte loss results in energy failure and eventually maturation arrest or death. Alternatively, it is tempting to speculate that oligodendrocyte maturation arrest may be connected to the apparent increase of the DNA-methylation marker 5-mc at 42 days of UP exposure, which is a very important repressor of gene transcription [42]. This theory is supported by several reports stating that changes in epigenetic regulatory mechanisms contribute to disturbed maturation and differentiation of immature oligodendrocytes [43-45]. Moreover, inflammation induced epigenetic changes during early development can cause substantial lasting neurodevelopmental impairments later in life [46, 47]. Altogether, these data

offer mechanistic insight in the association between intra-amniotic UP exposure and the increased incidence of adverse neurodevelopmental outcomes postnatally.

Interestingly, the cerebral phenotype following short term LPS exposure was remarkably different when compared to chronic UP exposure. In particular, we demonstrated that short term LPS exposure induced a rapid and temporal increase of the number of microglia and decreased myelin immunoreactivity, reflecting diffuse cerebral inflammation with hypomyelination. Microglia are important for inflammatory perinatal brain injury [43]. Aberrant or excessive microgliosis can be detrimental for the immature brain resulting in white matter injury [14], which corresponds to the loss of myelin that we found in our study. The cerebral inflammatory response following LPS in this study seems to be temporal since no increase in microglial density was found following 7d of LPS exposure. This dynamic response of activated microglia is consistent with distinct phases of cerebral inflammation [48] and can be explained by the presence of neutrophils in the choroid plexus, which are known to be important to the resolution of cerebral inflammation [26]. However, our immunohistochemical analysis does not rule out the possibility that phenotypic conversion of microglia might be induced following short term LPS or chronic UP exposure, which might influence the cerebral immune response.

Although such short time UP effects were not investigated in our model, in a study performed by Normann et al. [11] in rodents short term UP exposure during early pregnancy resulted in increased microglial density and decreased myelin basic protein density in the fetal brain. This cerebral phenotype is consistent with our data following short term LPS exposure indicating that timing and not the inflammatory trigger is more important in the neurological outcome of the fetal brain.

Besides the DNA-methylation marker 5-mc, the hydroxylated product and transcription activation marker 5-hmc was increased following 2d of LPS exposure. 5-hmc is very important for proper neurodevelopment and 5-hmc is altered in the umbilical cord of babies born after pre-eclampsia

and gestational diabetes mellitus [49] and in the hippocampus of 7-week old mice exposed to non-infectious stress [50]. In addition, 5-hmc alterations are associated with severe neurodevelopmental disorders such as Rett syndrome which is caused by mutations in the MeCP2 gene that encodes for proteins that directly bind to methylated DNA domains [51]. Therefore, the alterations we found in epigenetic markers following acute LPS exposure might explain, at least in part, the association between chorioamnionitis and the development of psychopathology later in life [52]. Since epigenetic changes are reversible, these findings provide new therapeutic targets to prevent long lasting neurodevelopmental morbidities following prenatal stress [17].

In addition, our lipid data provide supporting evidence that short-term LPS exposure results into lipid accumulation and "diseased" lipid patterns in the preterm brain. Such lipid accumulation in the brain is associated with severe neurological damage and altered brain functions [20]. In addition, we show a relative decrease of the myelin-specific sphingolipids in the white matter of the LPS exposed animals, which confirms and extends our findings concerning the loss of MBP in these animals. The abundance of phosphatidylinositols (PI) following 2d of LPS exposure was primarily seen within the region of increased IBA-1 IR. In line, the phosphorylated form of PI, phosphoinositide, is known to be upregulated in microglia and contributes to activation of microglia following ischemia [53].

Third, we found that chronic intra-amniotic UP exposure prevented an increase of IBA-1 IR and IBA-1+ cells, 5-hmc IR, lipid profile changes and a decrease of MBP IR upon a second inflammatory hit with LPS. This phenotype, also referred to as 'preconditioning', has been previously described in animal models in which pre-exposure to inflammation induced by LPS renders the brain less susceptible to a second hypoxic-ischemic insult, thereby resulting in less brain injury [54, 55]. This preconditioning effect of chronic UP exposure could be explained by work from Cao et al. [56] which showed in pregnant sheep that microglia once activated *in vivo* by

intra-amniotic LPS exposure, display diminished inflammatory responses following re-exposure to LPS. Moreover, they state that the memory acquired by microglia upon the first exposure to inflammation might be mediated by epigenetic regulatory processes [56]. Although this hypothesis needs to be tested in future studies, it is noteworthy that changes in the global level of 5-hmC and 5-mC were observed in our study following acute LPS exposure that was prevented by chronic UP exposure. Clearly, long term protection after inflammation induced preconditioning needs to be confirmed in a longitudinal study, but it is considered to be permanent since structural and functional protection up to 8 weeks was established following hypoxic preconditioning in a neonatal rodent model [57].

One important limitation of a large animal study is the relative low number of animals per group. Given the relative small animal numbers per group, we report actual p-values and tend to interpret p-values between 0.05 and 0.1 as biologically relevant. This assumption will decrease the chance of a false negative finding but increases the chance that one of these differences is a false positive result.

In this double-hit study, in which sequential different infectious hits were tested, we show that microbial interactions, the moment of onset and duration of these potential injurious triggers determine the neurological outcome. These findings seem to be an important explanation for the diversity of neurological outcomes associated with intra-amniotic UP exposure. Altogether, these data emphasize that an accurate history of infections during pregnancy is essential to guide neonatal management which warrants the need for biomarkers to diagnose antenatal infections.

Competing interest

The authors of this manuscript declare that there are no actual or potential conflicts of interest. The authors affirm that there are no financial, personal or other relationships with other people or organizations that have inappropriately influenced or biased their research.

Acknowledgements

This work was supported by National Institutes of Health (Bethesda, MD) grant (HD 57869), the Royal Society (London, UK) grant (IE130066) and by the Financial Markets Foundation for Children (Sydney, Australia) grant (EOI-2013–059). The authors would like to thank Nico Kloosterboer and Hellen Steinbusch for their excellent technical assistance.

References

1. Hagberg H, Gressens P, Mallard C. Inflammation during fetal and neonatal life: implications for neurologic and neuropsychiatric disease in children and adults. Annals of neurology. 2012;71(4):444-57. doi:10.1002/ana.22620.
2. Strunk T, Inder T, Wang X, Burgner D, Mallard C, Levy O. Infection-induced inflammation and cerebral injury in preterm infants. Lancet Infect Dis. 2014;14(8):751-62. doi:10.1016/S1473-3099(14)70710-8.
3. Rovira N, Alarcon A, Iriondo M, Ibanez M, Poo P, Cusi V et al. Impact of histological chorioamnionitis, funisitis and clinical chorioamnionitis on neurodevelopmental outcome of preterm infants. Early human development. 2011;87(4):253-7. doi:10.1016/j.earlhumdev.2011.01.024.
4. Kuypers E, Ophelders D, Jellema RK, Kunzmann S, Gavilanes AW, Kramer BW. White matter injury following fetal inflammatory response syndrome induced by chorioamnionitis and fetal sepsis: lessons from experimental ovine models. Early human development. 2012;88(12):931-6. doi:10.1016/j.earlhumdev.2012.09.011.
5. Sweeney EL, Kallapur SG, Gisslen T, Lambers DS, Chougnet CA, Stephenson SA et al. Placental Infection With Ureaplasma species Is Associated With Histologic Chorioamnionitis and Adverse Outcomes in Moderately Preterm and Late-Preterm Infants. The Journal of infectious diseases. 2016;213(8):1340-7. doi:10.1093/infdis/jiv587.
6. Viscardi RM. Ureaplasma species: role in diseases of prematurity. Clinics in perinatology. 2010;37(2):393-409. doi:10.1016/j.clp.2009.12.003.
7. Viscardi RM. Ureaplasma species: role in neonatal morbidities and outcomes. Archives of disease in childhood Fetal and neonatal edition. 2014;99(1):F87-92. doi:10.1136/archdischild-2012-303351.

8. Glaser K, Speer CP. Neonatal CNS infection and inflammation caused by Ureaplasma species: rare or relevant? Expert Rev Anti Infect Ther. 2015;13(2):233-48. doi:10.1586/14787210.2015.999670.
9. Kasper DC, Mechtler TP, Bohm J, Petricevic L, Gleiss A, Spergser J et al. In utero exposure to Ureaplasma spp. is associated with increased rate of bronchopulmonary dysplasia and intraventricular hemorrhage in preterm infants. J Perinat Med. 2011;39(3):331-6. doi:10.1515/JPM.2011.022.
10. Berger A, Witt A, Haiden N, Kaider A, Klebermasz K, Fuiko R et al. Intrauterine infection with Ureaplasma species is associated with adverse neuromotor outcome at 1 and 2 years adjusted age in preterm infants. J Perinat Med. 2009;37(1):72-8. doi:10.1515/JPM.2009.016.
11. Normann E, Lacaze-Masmonteil T, Eaton F, Schwendimann L, Gressens P, Thebaud B. A novel mouse model of Ureaplasma-induced perinatal inflammation: effects on lung and brain injury. Pediatric research. 2009;65(4):430-6. doi:10.1203/PDR.0b013e31819984ce.
12. Goldenberg RL, Andrews WW, Goepfert AR, Faye-Petersen O, Cliver SP, Carlo WA et al. The Alabama Preterm Birth Study: umbilical cord blood Ureaplasma urealyticum and Mycoplasma hominis cultures in very preterm newborn infants. American journal of obstetrics and gynecology. 2008;198(1):43 e1-5. doi:10.1016/j.ajog.2007.07.033.
13. Kirchner L, Helmer H, Heinze G, Wald M, Brunbauer M, Weninger M et al. Amnionitis with Ureaplasma urealyticum or other microbes leads to increased morbidity and prolonged hospitalization in very low birth weight infants. Eur J Obstet Gynecol Reprod Biol. 2007;134(1):44-50. doi:10.1016/j.ejogrb.2006.09.013.
14. Jin C, Londono I, Mallard C, Lodygensky GA. New means to assess neonatal inflammatory brain injury. Journal of neuroinflammation. 2015;12:180. doi:10.1186/s12974-015-0397-2.
15. Hagberg H, Dammann O, Mallard C, Leviton A. Preconditioning and the developing brain. Semin Perinatol. 2004;28(6):389-95.
16. Fleiss B, Tann CJ, Degos V, Sigaut S, Van Steenwinckel J, Schang AL et al. Inflammation-induced sensitization of the brain in term infants. Developmental medicine and child neurology. 2015;57 Suppl 3:17-28. doi:10.1111/dmcn.12723.
17. Gao Q, Tang J, Chen J, Jiang L, Zhu X, Xu Z. Epigenetic code and potential epigenetic-based therapies against chronic diseases in developmental origins. Drug discovery today. 2014;19(11):1744-50. doi:10.1016/j.drudis.2014.05.004.
18. Liu Y, Hoyo C, Murphy S, Huang Z, Overcash F, Thompson J et al. DNA methylation at imprint regulatory regions in preterm birth and infection. American journal of obstetrics and gynecology. 2013;208(5):395 e1-7. doi:10.1016/j.ajog.2013.02.006.
19. Farooqui AA, Horrocks LA, Farooqui T. Glycerophospholipids in brain: their metabolism, incorporation into membranes, functions, and involvement in neurological disorders. Chemistry and physics of lipids. 2000;106(1):1-29.
20. Adibhatla RM, Hatcher JF. Role of Lipids in Brain Injury and Diseases. Future lipidology. 2007;2(4):403-22. doi:10.2217/17460875.2.4.403.
21. Miura Y, Payne MS, Keelan JA, Noe A, Carter S, Watts R et al. Maternal intravenous treatment with either azithromycin or solithromycin clears Ureaplasma parvum from the amniotic fluid in an ovine model of intrauterine infection. Antimicrobial agents and chemotherapy. 2014;58(9):5413-20. doi:10.1128/AAC.03187-14.

22. Gavilanes AW, Strackx E, Kramer BW, Gantert M, Van den Hove D, Steinbusch H et al. Chorioamnionitis induced by intraamniotic lipopolysaccharide resulted in an interval-dependent increase in central nervous system injury in the fetal sheep. American journal of obstetrics and gynecology. 2009;200(4):437 e1-8. doi:10.1016/j.ajog.2008.12.003.
23. Hankin JA, Farias SE, Barkley RM, Heidenreich K, Frey LC, Hamazaki K et al. MALDI mass spectrometric imaging of lipids in rat brain injury models. Journal of the American Society for Mass Spectrometry. 2011;22(6):1014-21. doi:10.1007/s13361-011-0122-z.
24. Jellema RK, Lima Passos V, Zwanenburg A, Ophelders DR, De Munter S, Vanderlocht J et al. Cerebral inflammation and mobilization of the peripheral immune system following global hypoxia-ischemia in preterm sheep. Journal of neuroinflammation. 2013;10:13. doi:10.1186/1742-2094-10-13.
25. Lardenoije R, van den Hove DLA, Vaessen TSJ, Iatrou A, Meuwissen KPV, van Hagen BTJ et al. Epigenetic modifications in mouse cerebellar Purkinje cells: effects of aging, caloric restriction, and overexpression of superoxide dismutase 1 on 5-methylcytosine and 5-hydroxymethylcytosine. Neurobiology of aging. 2015;36(11):3079-89. doi:10.1016/j.neurobiolaging.2015.08.001.
26. Schwartz M, Baruch K. The resolution of neuroinflammation in neurodegeneration: leukocyte recruitment via the choroid plexus. The EMBO journal. 2014;33(1):7-22. doi:10.1002/embj.201386609.
27. Chen Y, Ozturk NC, Zhou FC. DNA methylation program in developing hippocampus and its alteration by alcohol. PloS one. 2013;8(3):e60503. doi:10.1371/journal.pone.0060503.
28. Wang Z, Tang B, He Y, Jin P. DNA methylation dynamics in neurogenesis. Epigenomics. 2016;8(3):401-14. doi:10.2217/epi.15.119.
29. Veloso A, Astigarraga E, Barreda-Gomez G, Manuel I, Ferrer I, Giralt MT et al. Anatomical distribution of lipids in human brain cortex by imaging mass spectrometry. Journal of the American Society for Mass Spectrometry. 2011;22(2):329-38. doi:10.1007/s13361-010-0024-5.
30. Carter CL, McLeod CW, Bunch J. Imaging of phospholipids in formalin fixed rat brain sections by matrix assisted laser desorption/ionization mass spectrometry. Journal of the American Society for Mass Spectrometry. 2011;22(11):1991-8. doi:10.1007/s13361-011-0227-4.
31. Angerer TB, Dowlatshahi Pour M, Malmberg P, Fletcher JS. Improved molecular imaging in rodent brain with time-of-flight-secondary ion mass spectrometry using gas cluster ion beams and reactive vapor exposure. Analytical chemistry. 2015;87(8):4305-13. doi:10.1021/ac504774y.
32. Carson MJ, Thrash JC, Walter B. The cellular response in neuroinflammation: The role of leukocytes, microglia and astrocytes in neuronal death and survival. Clinical neuroscience research. 2006;6(5):237-45. doi:10.1016/j.cnr.2006.09.004.
33. Burd I, Brown A, Gonzalez JM, Chai J, Elovitz MA. A mouse model of term chorioamnionitis: unraveling causes of adverse neurological outcomes. Reproductive sciences. 2011;18(9):900-7. doi:10.1177/1933719111398498.
34. Yang Y, Higashimori H, Morel L. Developmental maturation of astrocytes and pathogenesis of neurodevelopmental disorders. Journal of neurodevelopmental disorders. 2013;5(1):22. doi:10.1186/1866-1955-5-22.
35. Sharma R, Fischer MT, Bauer J, Felts PA, Smith KJ, Misu T et al. Inflammation induced by innate immunity in the central nervous system leads to primary astrocyte

dysfunction followed by demyelination. Acta neuropathologica. 2010;120(2):223-36. doi:10.1007/s00401-010-0704-z.
36. Bonestroo HJ, Heijnen CJ, Groenendaal F, van Bel F, Nijboer CH. Development of cerebral gray and white matter injury and cerebral inflammation over time after inflammatory perinatal asphyxia. Developmental neuroscience. 2015;37(1):78-94. doi:10.1159/000368770.
37. Volpe JJ. Neurobiology of periventricular leukomalacia in the premature infant. Pediatric research. 2001;50(5):553-62. doi:10.1203/00006450-200111000-00003.
38. Penn AA, Gressens P, Fleiss B, Back SA, Gallo V. Controversies in preterm brain injury. Neurobiology of disease. 2016;92(Pt A):90-101. doi:10.1016/j.nbd.2015.10.012.
39. Segovia KN, McClure M, Moravec M, Luo NL, Wan Y, Gong X et al. Arrested oligodendrocyte lineage maturation in chronic perinatal white matter injury. Annals of neurology. 2008;63(4):520-30. doi:10.1002/ana.21359.
40. Back SA, Miller SP. Brain injury in premature neonates: A primary cerebral dysmaturation disorder? Annals of neurology. 2014;75(4):469-86. doi:10.1002/ana.24132.
41. Kamasawa N, Sik A, Morita M, Yasumura T, Davidson KG, Nagy JI et al. Connexin-47 and connexin-32 in gap junctions of oligodendrocyte somata, myelin sheaths, paranodal loops and Schmidt-Lanterman incisures: implications for ionic homeostasis and potassium siphoning. Neuroscience. 2005;136(1):65-86. doi:10.1016/j.neuroscience.2005.08.027.
42. Ficz G, Branco MR, Seisenberger S, Santos F, Krueger F, Hore TA et al. Dynamic regulation of 5-hydroxymethylcytosine in mouse ES cells and during differentiation. Nature. 2011;473(7347):398-402. doi:10.1038/nature10008.
43. Fleiss B, Gressens P. Tertiary mechanisms of brain damage: a new hope for treatment of cerebral palsy? The Lancet Neurology. 2012;11(6):556-66. doi:10.1016/S1474-4422(12)70058-3.
44. Favrais G, van de Looij Y, Fleiss B, Ramanantsoa N, Bonnin P, Stoltenburg-Didinger G et al. Systemic inflammation disrupts the developmental program of white matter. Annals of neurology. 2011;70(4):550-65. doi:10.1002/ana.22489.
45. van Tilborg E, Heijnen CJ, Benders MJ, van Bel F, Fleiss B, Gressens P et al. Impaired oligodendrocyte maturation in preterm infants: Potential therapeutic targets. Progress in neurobiology. 2016;136:28-49. doi:10.1016/j.pneurobio.2015.11.002.
46. Jirtle RL, Skinner MK. Environmental epigenomics and disease susceptibility. Nature reviews Genetics. 2007;8(4):253-62. doi:10.1038/nrg2045.
47. Bilbo SD, Schwarz JM. Early-life programming of later-life brain and behavior: a critical role for the immune system. Frontiers in behavioral neuroscience. 2009;3:14. doi:10.3389/neuro.08.014.2009.
48. Hagberg H, Mallard C, Ferriero DM, Vannucci SJ, Levison SW, Vexler ZS et al. The role of inflammation in perinatal brain injury. Nature reviews Neurology. 2015;11(4):192-208. doi:10.1038/nrneurol.2015.13.
49. Sun M, Song MM, Wei B, Gao Q, Li L, Yao B et al. 5-Hydroxymethylcytosine-mediated alteration of transposon activity associated with the exposure to adverse in utero environments in human. Human molecular genetics. 2016. doi:10.1093/hmg/ddw089.
50. Li S, Papale LA, Kintner DB, Sabat G, Barrett-Wilt GA, Cengiz P et al. Hippocampal increase of 5-hmC in the glucocorticoid receptor gene following acute stress. Behavioural brain research. 2015;286:236-40. doi:10.1016/j.bbr.2015.03.002.

51. Szulwach KE, Li X, Li Y, Song CX, Wu H, Dai Q et al. 5-hmC-mediated epigenetic dynamics during postnatal neurodevelopment and aging. Nature neuroscience. 2011;14(12):1607-16. doi:10.1038/nn.2959.
52. Meyer U. Prenatal poly(i:C) exposure and other developmental immune activation models in rodent systems. Biological psychiatry. 2014;75(4):307-15. doi:10.1016/j.biopsych.2013.07.011.
53. Jin R, Yu S, Song Z, Quillin JW, Deasis DP, Penninger JM et al. Phosphoinositide 3-kinase-gamma expression is upregulated in brain microglia and contributes to ischemia-induced microglial activation in acute experimental stroke. Biochemical and biophysical research communications. 2010;399(3):458-64. doi:10.1016/j.bbrc.2010.07.116.
54. Eklind S, Mallard C, Arvidsson P, Hagberg H. Lipopolysaccharide induces both a primary and a secondary phase of sensitization in the developing rat brain. Pediatric research. 2005;58(1):112-6. doi:10.1203/01.PDR.0000163513.03619.8D.
55. Mallard C, Hagberg H. Inflammation-induced preconditioning in the immature brain. Seminars in fetal & neonatal medicine. 2007;12(4):280-6. doi:10.1016/j.siny.2007.01.014.
56. Cao M, Cortes M, Moore CS, Leong SY, Durosier LD, Burns P et al. Fetal microglial phenotype in vitro carries memory of prior in vivo exposure to inflammation. Frontiers in cellular neuroscience. 2015;9:294. doi:10.3389/fncel.2015.00294.
57. Gustavsson M, Anderson MF, Mallard C, Hagberg H. Hypoxic preconditioning confers long-term reduction of brain injury and improvement of neurological ability in immature rats. Pediatric research. 2005;57(2):305-9. doi:10.1203/01.PDR.0000151122.58665.70.

Figure legends

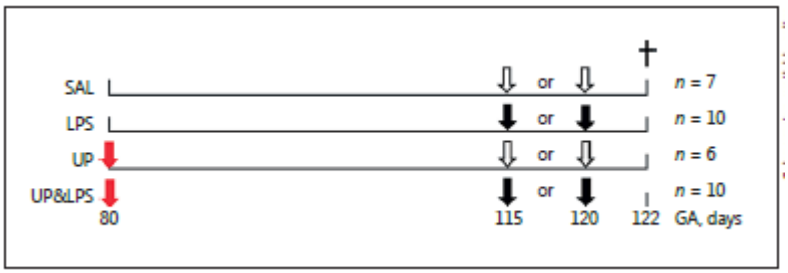

Figure 1 Experimental groups. Animals were intra-amniotically exposed to *Ureaplasma parvum* (UP; red arrow) for 42 days with (n=11) or without (n=6) subsequent lipopolysaccharide (LPS; black arrow) exposure at 2 (n=5) or 7 (n=5) days before preterm delivery at 122 days of gestation (GA) and sacrificed immediately after birth (†). Control animals received intra-amniotic injection with saline (SAL; open arrow)

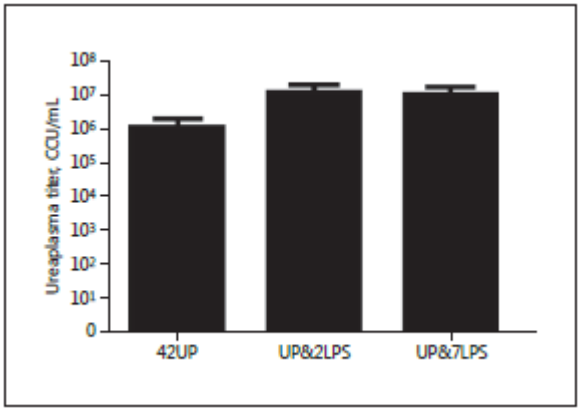

Figure 2 Ureaplasma titer at time of subsequent LPS or saline injection. Establishment of chronic infection was confirmed in amniocentesis samples taken at time of LPS or saline injection. Mean and standard error of the mean are shown for each group (culture titration of viable UP determined in triplicate for each animal). No statistical difference was found by one-way ANOVA testing

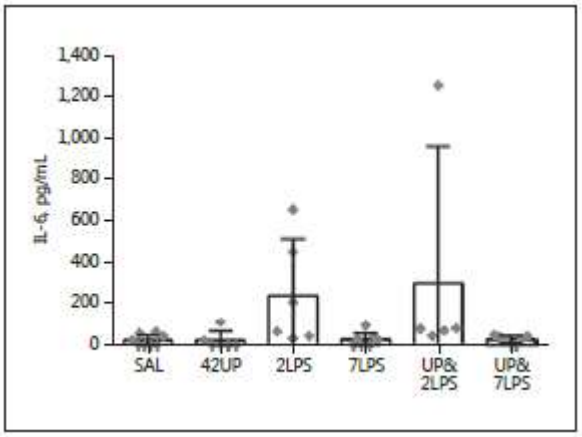

Figure 3 Systemic immune activation was ascertained by measuring circulatory IL-6 concentrations. For statistical analysis, undetectable values were assigned an arbitrary value of 1 pg/mL. No statistical difference was found by one-way ANOVA testing

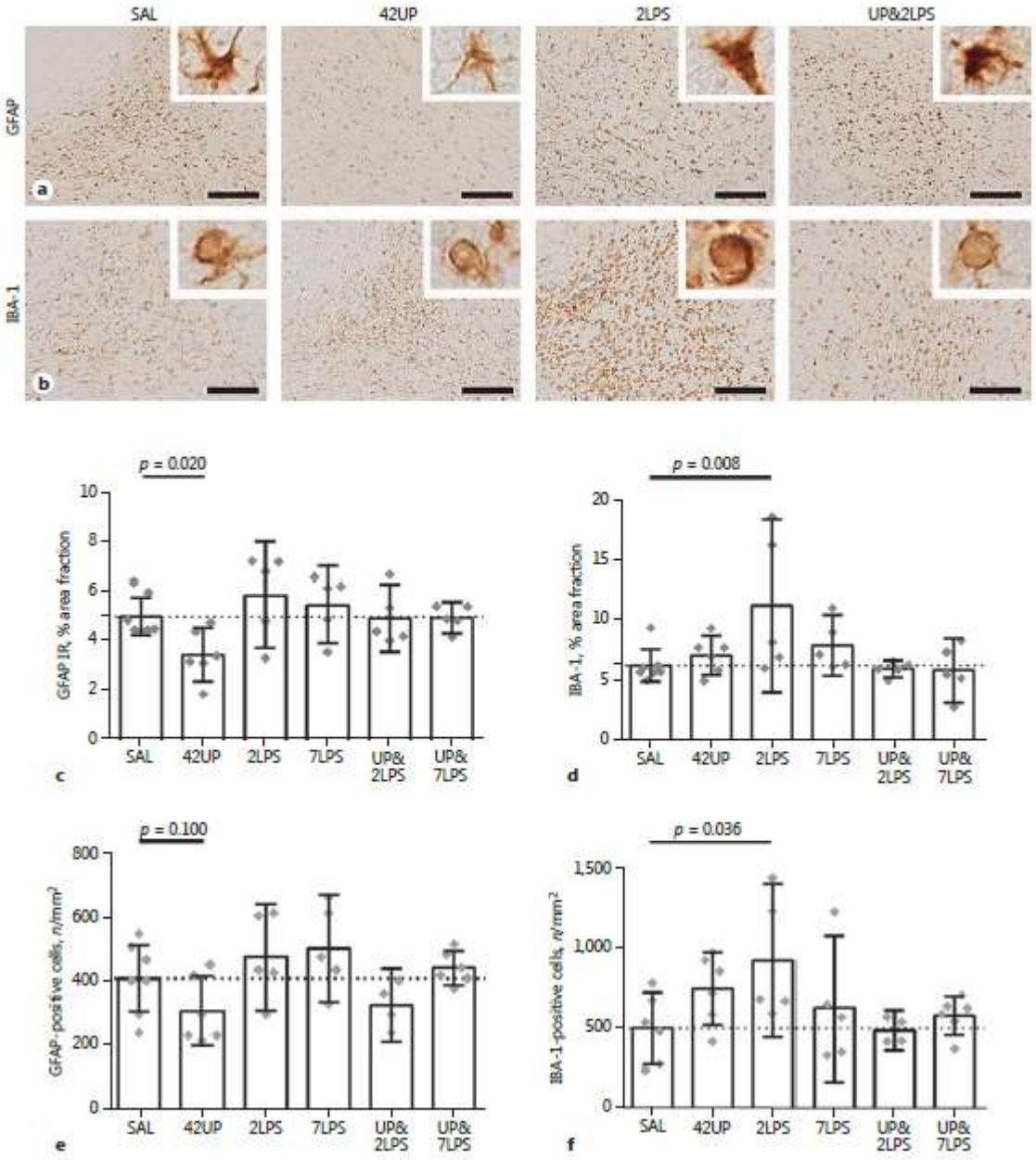

Figure 4 Intra-amniotic exposure to Ureaplasma parvum (UP) induces a decrease of astrocytes and preconditions the fetal brain against re-exposure to lipopolysaccharide (LPS). A significant decrease (*, $p<0.05$) of the area fraction of GFAP immunoreactivity (IR) was observed in animals of the chronic UP group (42UP) compared to controls (SAL) (SAL vs. 42UP; $p=0.020$) (**a & c**). GFAP positive cells tended to be decreased following chronic UP exposure

(SAL vs. 42UP; p = 0.100) (**e**). No changes in GFAP IR were found in animals of the LPS exposed groups regardless of the presence or absence of UP pre-exposure. Significant increase (*, $p<0.05$) of the area fraction of IBA-1 IR and IBA-1 positive cells was observed in animals of the 2 d LPS group (2LPS) (SAL vs. 2LPS; p = 0.008 and p = 0.036 respectively) which was prevented by pre-exposure to UP (UP&2LPS) (**b & d & f**). No changes of IBA-1 IR and cell numbers were found in animals of the 7 d LPS group (SAL vs. 7LPS; p = 0.342 and p = 1.00 respectively) (**d & f**). Representative histological figures of the GFAP positive astrocytes and IBA-1 positive microglia are shown in (**a**) and (**b**) respectively. Morphological analysis showed a higher density of amoeboid microglia present in the white matter after 2 days of LPS exposure (**b**, inserts). Figures of animals of the 7 d LPS group (7LPS) and 42 d UP and 7 d LPS group (UP&7LPS) are not depicted. GFAP and IBA-1 IR are represented in the graphs as mean % area fraction ± 95% CI. Images taken at 100x magnification (insert at 400x magnification), scale bar = 200 µm

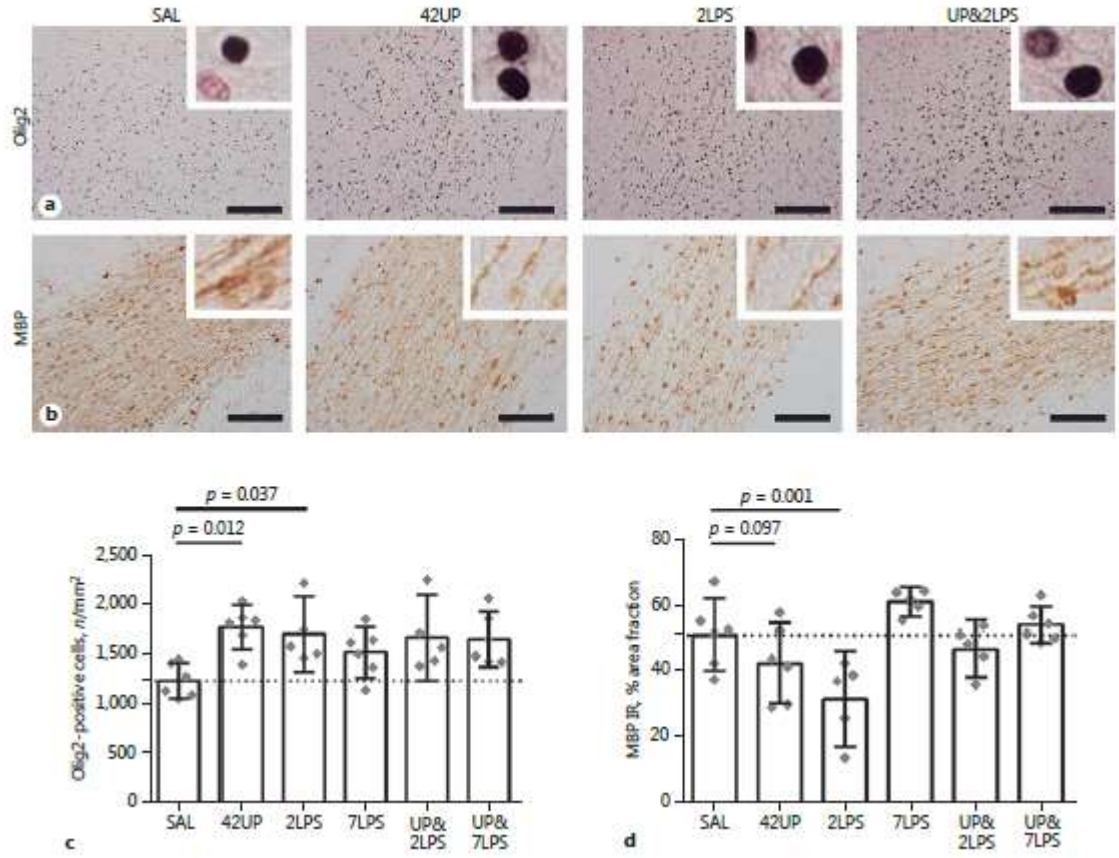

Figure 5 Intra-amniotic exposure to Ureaplasma parvum (UP) induces changes in white matter development and preconditions the fetal brain upon re-exposure to a second inflammatory hit with lipopolysaccharide (LPS). Significant increase (*, p<0.05) of Olig2 positive cells was observed in animals of the chronic UP group (SAL vs. 42UP; p = 0.012) and of the 2d LPS group (SAL vs. 2 LPS; p = 0.037) compared to controls (**b & c**). This increase of Olig2 positive cells was accompanied by a decrease in MBP (SAL vs. 42UP; p = 0.097 and SAL vs. 2LPS; p = 0.001) (**a & d**). This decrease of MBP IR was prevented in the short term LPS exposed animals that were pre-exposed to UP. At 7d of LPS exposure no changes in MBP IR were found (2LPS vs. 7LPS; p = 0.000). Olig2 is represented as mean positive cells/mm2 ± 95% CI and MBP IR is represented in the graphs as mean % area fraction ± 95% CI. Images taken at 100x magnification (insert at 400x magnification), scale bar= 200 µm

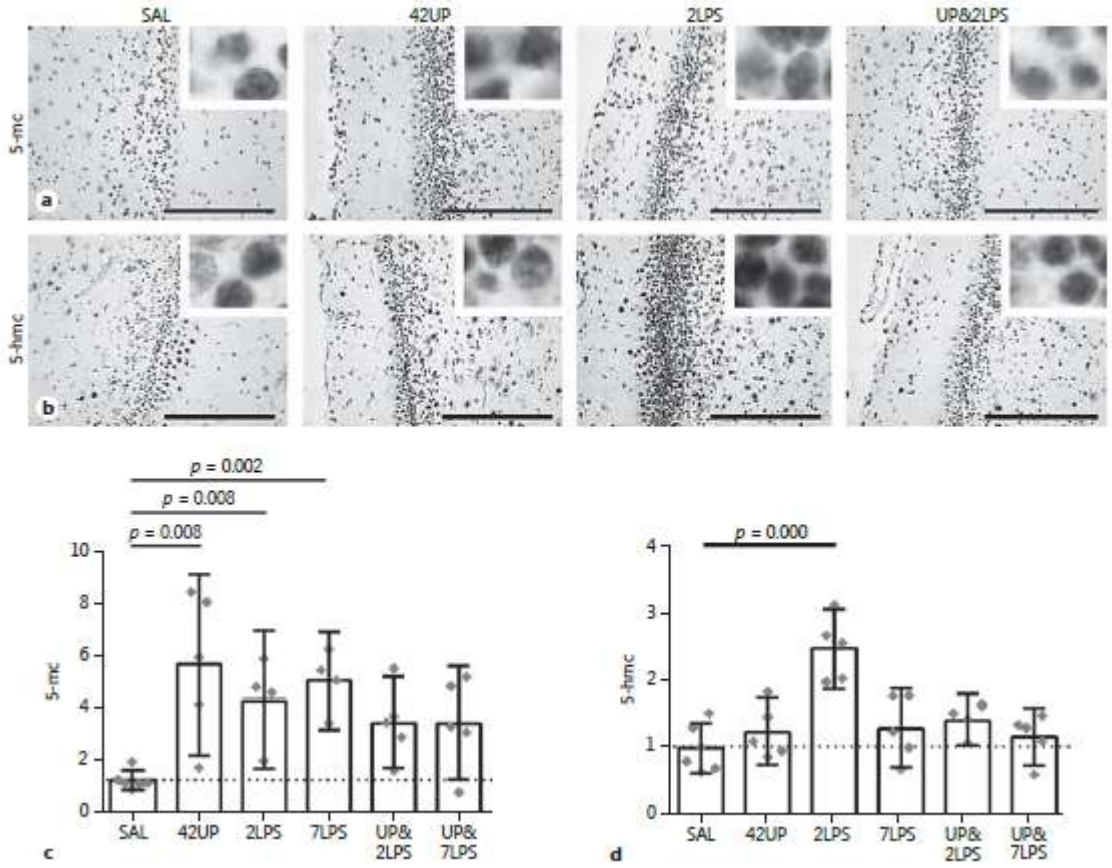

Figure 6 Changes of the epigenetic markers 5-mc and 5-hmc following intra-amniotic exposure to Ureaplasma parvum (UP) and short-term exposure to lipopolysaccharide (LPS) in the dentate gyrus of the hippocampus. Significant increase (*, $p<0.05$) of the gene repression marker 5-mc IR was observed in short term LPS exposed animals and chronic UP exposed animals when compared to controls (SAL vs. 2LPS; $p = 0.008$ and SAL vs. 7LPS; $p = 0.002$ and SAL vs. 42UP; $p = 0.008$) (**a & c**). Significant increase (*, $p<0.05$) in transcription activation marker 5-hmc IR was restricted to the 2d LPS group compared to controls (SAL vs. 2LPS; $p = 0.000$; 2LPS vs. 7LPS; $p = 0.000$), which was prevented by pre-exposure to UP. 5-mc and 5-hmc are represented in the graphs as mean integrated density ± 95% CI. The integrated density was calculated by multiplying the area fraction and gray intensity measurements. Values were normalized to the data

of the control group. Images taken at 200x magnification (insert at 400x magnification), scale bar= 200 µm

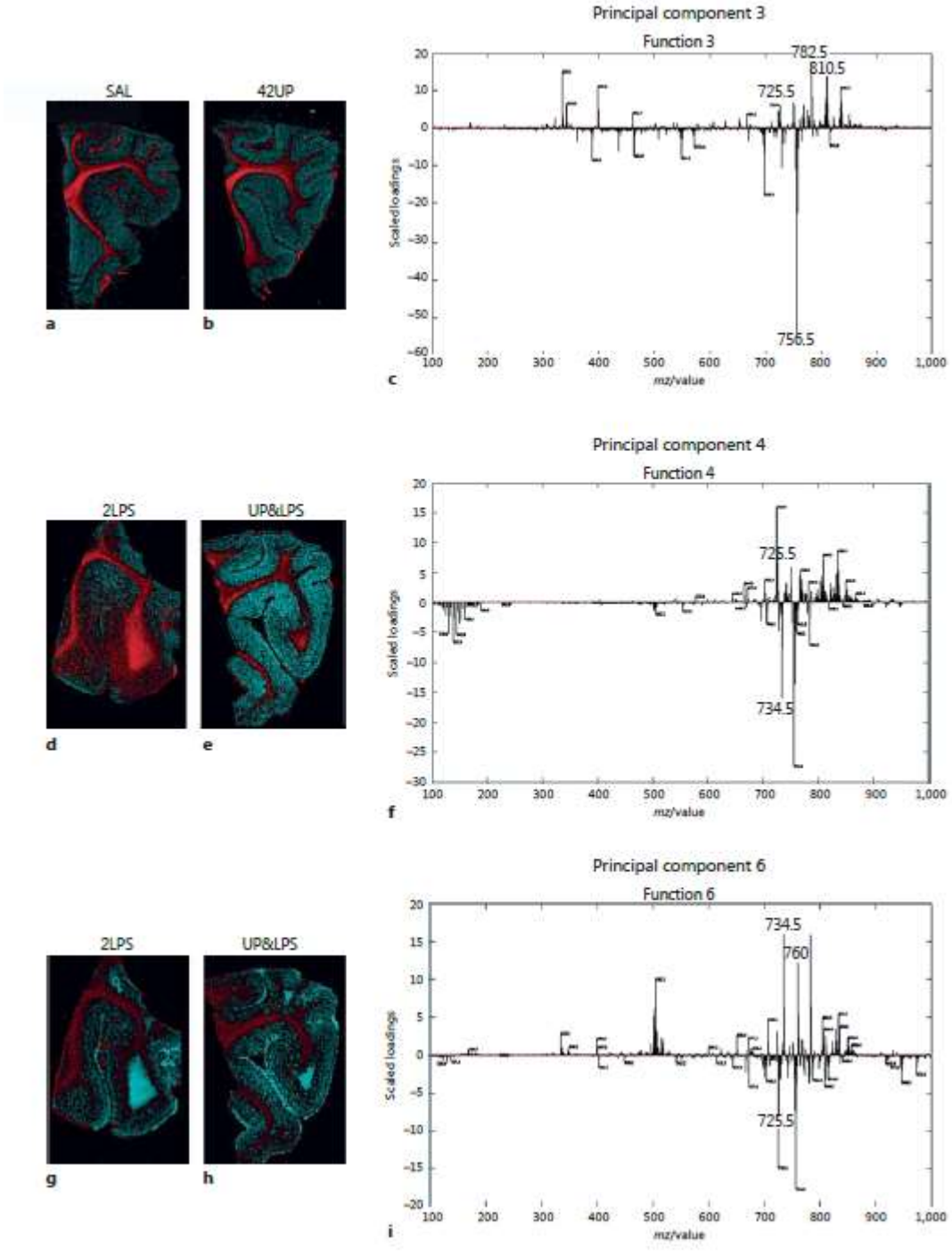

Figure 7 Matrix assisted laser desorption ionization mass spectrometry imaging (MALDI-MSI) performed in positive ion mode followed by principal component analysis (PCA). a shows the reconstructed image that represents the molecular differences of lipids between white (red area) and grey matter (green area) of control and UP animals. PCA 3 demonstrates similar lipid compositions of white and grey matter of control and UP animals (**a-c**). In particular, phosphocholine (PC) species m/z 782.5 PC 34:1+Na+, m/z 810.5 PC 36:1+Na+ or sphingomyelin m/z 725.5 SM 34:1+Na+ are present in white matter (positive spectrum principal component 3) whereas PC m/z 756.5 32:0+Na+ is present in grey matter of control and 42UP animals (negative spectrum principal component 3). Short-term LPS exposure results in lipid accumulation in the white matter as illustrated by an increased intensity of the white matter related peaks, especially m/z 725.5 (**d & g**) (positive spectrum of principal component 4). In addition, a shift of white and grey matter specific molecular patterns is observed at 2d LPS exposure illustrated by more white matter specific lipids present in the grey matter such as m/z 725.5 (**d**, negative spectrum of principal component 6); and grey matter specific lipids into the white matter such as m/z 734.5 PC 32:0+H+ and m/z 760 PC 34:1+H+ (**g**, positive spectrum of principal component 6). These changes were prevented by pre-exposure to UP (**e & h**)

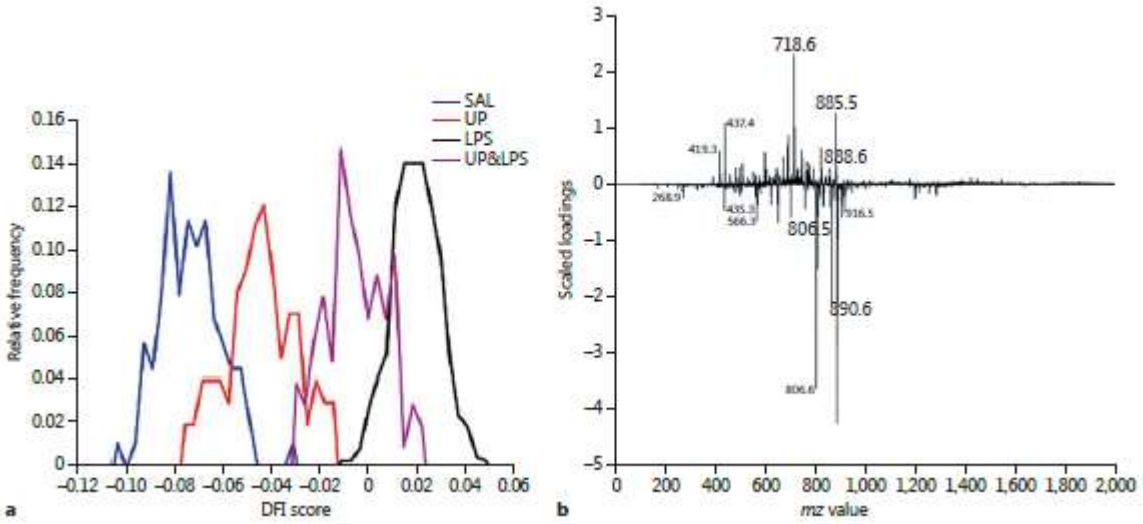

Figure 8 Matrix assisted laser desorption ionization mass spectrometry imaging (MALDI-MSI) performed in negative ion mode followed by PCA. The DF1 (**a**) revealed that the highest differences were observed between the control (negative scores) and LPS group (positive scores). Both 42UP and UP&LPS groups had negative scores which were comparable to the control group. The DF1 spectrum of the 2 days of LPS exposed animals (**b**) showed that LPS infection reduced the amount of sulfatide (SF) species such as m/z 806.5 SF 18:0-H-, m/z 888.6 SF 24:1-H-, m/z 890.6 SF 24:0-H-. These species were mainly present in the white matter of control, UP and UP&LPS groups (spectrum not shown) whereas m/z 885.5 PI 38:4-H- or m/z 718.6 PC 31:0-H- were representative of the white matter in animals of the 2LPS group (**b**)

Tables

	SAL (n=7)	42UP (n=6)	2LPS (N=5)	7LPS (N=5)	UP&2LPS (N= 5)	UP&7LPS (n= 5)
Body weight (g)	3021 ± 328	2765 ± 312	2256 ± 305*	3040 ± 285	2580 ± 285	2652 ± 396
Brain weight (g)	52.2 ± 4.5	50.8 ± 4.9	46.0 ± 2.8$^{\#}$	51.7 ± 7.0	47.9 ± 2.1	51.7 ± 4.1
Brain/body Ratio (%)	1.7 ± 0.02	1.9 ± 0.02	2.1 ± 0.02*	1.7 ± 0.02	1.9 ± 0.02	2.0 ± 0.02

Table 1 Animal characteristics.

Animal characteristics are expressed as mean (±SD). One-way ANOVA with Dunnett's multiple comparison testing was performed. * $p < 0.05$ versus control; $^{\#}$ $p < 0.1$ versus control

Table 2 Immune cells present in the choroid plexus.

cells/mm^2	SAL (n=7)	42UP (n=6)	2LPS (N=5)	7LPS (N=5)	UP&2LPS (N= 5)	UP&7LPS (n= 5)
MPO+ cells	3.31±2.72	6.80±10.29	8.58±2.84	14.66±8.96$^{\#}$	1.06±0.87	5.68±9.36
CD68+ cells	67.99±47.40	48.45±33.92	69.91±51.64	80.62±32.07	64.49±49.05	59.31±40.18
CD3+ cells	28.98±24.96	11.14±7.21	30.82±34.98	47.24±23.73	26.11±35.25	15.92±19.32

Cell counts of MPO+, CD68+ and CD3+ cells in the choroid plexus are expressed as cells/mm^2 (±SD). One-way ANOVA with Dunnett's multiple comparison testing was performed. * $p < 0.05$ versus control; $^{\#}$ $p < 0.1$ versus control